THE JOURNAL OF BIOLOGICAL CHEMISTRY
Vol. 274, No. 53, Issue of December 31, pp. 37915–37922, 1999
Printed in U.S.A.


# Subcellular Compartmentalization of Activation and Desensitization of Responses Mediated by NK2 Neurokinin Receptors*

(Received for publication, August 9, 1999, and in revised form, September 24, 1999)

**Jean-Yves Vollmer‡§, Philippe Alix‡¶, André Chollet‖, Kenneth Takeda**, and Jean-Luc Galzi‡§§**

*From the ‡Département Récepteurs et Protéines Membranaires, CNRS UPR 9050, Ecole Supérieure de Biotechnologie de Strasbourg, Boulevard Sébastien Brant, 67400 Illkirch, France, ‖Serono Pharmaceutical Research Institute, 14 chemin des Aulx, CH-1228 Plan-les-Ouates/Genève, Switzerland, and **Pharmacologie et Physicochimie des Interactions Cellulaires et Moléculaires, CNRS UMR 7034, Université Louis Pasteur de Strasbourg, Faculté de Pharmacie, B.P. 24, 67401 Illkirch, France*

**A functional fluorescent neurokinin NK2 receptor was constructed by joining enhanced green fluorescent protein to the amino-terminal end of the rat NK2 receptor and was expressed in human embryonic kidney cells. On cell suspensions, the binding of fluorescent Bodipy-labeled neurokinin A results in a saturatable and reversible decrease of NK2 receptor fluorescence via fluorescence resonance energy transfer. This can be quantified for nM to μM agonist concentrations and monitored in parallel with intracellular calcium responses. On single cells, receptor site occupancy and local agonist concentration can be determined in real time from the decrease in receptor fluorescence. Simultaneous measurement of intracellular calcium responses and agonist binding reveals that partial receptor site occupancy is sufficient to desensitize cellular response to a second agonist application to the same membrane area. Subsequent stimulation of a distal membrane area leads to a second response to agonist, provided that it had not been exposed to agonist during the first application. Together with persistent translocation of fluorescent protein kinase C to the membrane area exposed to agonist, the present data support that not only homologous desensitization but also heterologous desensitization of NK2 receptors is compartmentalized to discrete membrane domains.**

Neurotransmitters stimulate target cells upon interacting with two major categories of regulatory proteins, ligand-gated ion channels (1–3), and G protein-coupled receptors (4). For ligand-gated ion channels, response activation and termination are mediated by a single molecule that carries the neurotransmitter site and the effector site (1). In contrast, responses mediated by G protein-coupled receptors result from a complex cascade of transient and sequential interactions between the receptor and a series of distinct messengers and effector proteins, which belong to distinct subcellular compartments (5–9).

Tachykinins or neurokinins form a family of related neuropeptides found throughout central and peripheral nervous tissues. Their biological activities related to pain transmission (10, 11), smooth muscle contraction, vasodilation, or neurogenic inflammation are mediated by at least three distinct G protein-coupled receptors, NK1, NK2, and NK3, that show preferential binding for the endogenous agonists substance P, neurokinin A (NKA),[1] and neurokinin B (NKB), respectively (12). All three receptor isotypes belong to the family of seven transmembrane regulatory proteins and are coupled to an intracellular calcium release response primarily mediated by the pertussis toxin-insensitive heterotrimeric GTP-binding protein Gq/G11.

In the present work, we have used fluorescence resonance energy transfer-based detection of neurokinin A binding to its G protein-coupled receptor, the NK2 tachykinin receptor, to detect real-time interactions on living cells and to study the spatial distribution of response activation and desensitization at the single cell level. Tachykinin NK2 receptors were fluorescently labeled at the amino-terminal end with EGFP and expressed as functional membrane-bound receptors in HEK 293 cells. The binding of the natural neuropeptide neurokinin A chemically labeled with the fluorophore Bodipy 530/550 can be monitored by fluorescence resonance energy transfer and quantified both on cell suspensions and single cells. Real time ligand binding with high spatial resolution was measured in single cells, thereby permitting investigation of the relationships between the distribution of receptor activation/desensitization and cellular responses.

## EXPERIMENTAL PROCEDURES

*cDNA Constructs, Expression, and Selection*—Rat NK2R cDNA (56) was provided by Prof. S. Nakanishi (Kyoto University), α7-5HT3 cDNA (57) in KS vector was provided by Prof. J. P. Changeux (Institut Pasteur, Paris, France), PKCα-EGFP in pEGFP-C1 vector was obtained from Dr. D. Joubert (INSERM U469, Montpellier, France). The α7-5HT3 sequence was excised from the plasmid by the restriction enzymes *Bsr*GI and *Xho*I leaving the α7 signal sequence (*Not*I-*Bsr*GI fragment) linked to the KS vector. EGFP (pEGFP-C3, CLONTECH) was mutated to introduce an additional *Bsr*GI site (Sculptor site-directed mutagenesis kit, Amersham Pharmacia Biotech) on its translation initiation codon and cloned in frame with the signal sequence as a *Bsr*GI-*Xho*I fragment (KS-sp-EGFP). NK2R cDNA in vector SK was subcloned in vector KS between the *Spe*I (5′-end) and *Xho*I (3′-end) sites. The large *Xho*I fragment was then cloned in the *Xho*I site of KS-sp-EGFP to yield chimera 1. Chimera 2 was obtained after introducing an *Xho*I site on nucleotide 99 of the NK2R coding sequence, to permit in frame fusion with EGFP. All constructs were then ligated in

* This work was supported by the Centre National de la Recherche Scientifique, the Association pour la Recherche sur le Cancer, the Fondation pour le Recherche Médicale, the Ligue Nationale Contre le Cancer (Comité du Haut-Rhin), the Communauté Urbaine de Strasbourg, and the Université Louis Pasteur de Strasbourg. The costs of publication of this article were defrayed in part by the payment of page charges. This article must therefore be hereby marked "*advertisement*" in accordance with 18 U.S.C. Section 1734 solely to indicate this fact.

§ Recipient of a fellowship from the Agence Nationale pour la Recherche sur le SIDA.

¶ Present address: Laboratoire de Neurophysiologie (RCIM), Université d'Angers, rue Haute de Reculée, 49045 Angers Cedex, France.

§§ To whom correspondence should be addressed: Tel.: (33) 3 88 65 52 93; Fax: (33) 3 88 65 52 98; E-mail: galzi@esbs.u-strasbg.fr.

[1] The abbreviations used are: NKA and NKB, neurokinin A and B; Bo, Bodipy 530/550; EGFP, enhanced green fluorescent protein; sp, signal peptide; WT, wild type; PKC, protein kinase C.

the expression vector pCEP4 (Invitrogen) between the *Not*I and *Xho*I sites for expression in HEK 293 cells.

HEK 293 cells, grown in minimal essential medium complemented with 10% fetal calf serum and antibiotics, were transfected by calcium phosphate precipitation (58) and selected with 500 or 4000 $\mu$g/ml hygromycin B.

*Radioligand Binding Experiments*—All peptides used were obtained from Bachem. [$^3$H]SR48968 (Amersham Pharmacia Biotech) binding was performed on intact cells (25,000 cells/500 $\mu$l) in Hepes buffer (137.5 mM NaCl, 1.25 mM $MgCl_2$, 1.25 mM $CaCl_2$, 6 mM KCl, 5.6 mM glucose, 10 mM Hepes, 0.4 mM $NaH_2PO_4$, 1% mM bovine serum albumin (w/v), pH 7.4) supplemented with protease inhibitors (Complete TM, Roche Molecular Biochemicals) at 4 °C for 2 h. Samples were filtered through GF/C filters preincubated with 1% (w/v) milk powder in phosphate-buffered saline (137.5 mM NaCl, 2.68 mM KCl, 8.06 mM $Na_2HPO_4$, 1.47 mM $KH_2PO_4$) and rinsed twice with phosphate-buffered saline. Competition experiments were performed with 0.5–1 nM [$^3$H]SR48968, and experimental $IC_{50}$ values were converted to $K_i$ values using the Cheng and Prusoff relation (59). SR48968 was kindly given by Dr. Emonds-Alt (60). For inhibition of [$^{125}$I]NKA binding experiments, $K_i$ values were determined by taking $K_D$ = 1 nM for NKA (14).

*Synthesis of Fluorescent NKA*—All reactants are dissolved in dimethylformamide. Neurokinin A (0.2 $\mu$mol) was mixed with 0.4 $\mu$mol of iodoacetyl-Bodipy 530/550 (Molecular Probes) and 0.8 $\mu$mol of triethylamine. The volume was adjusted to 100 $\mu$l with dimethylformamide, stirred, and allowed to stand at room temperature for 16 h. The reaction mixture was then applied to a reverse phase high pressure liquid chromatography column (Zorbax Z5C8 25F) equilibrated with 90% A (0.1% trifluoroacetic acid in $H_2O$) 10% solvent B (0.1% trifluoroacetic acid in acetonitrile) and eluted at 1 ml/min using a 10–95% gradient of solvent B in 60 min. Elution was monitored by optical absorption at 219 and 530 nm. The product eluting at 34 min, which exhibits strong absorption at both wavelength, was collected, concentrated, and characterized as the mono-Bodipy 530/550 derivative of neurokinin A (designated NKA-Bo) by spectrofluorimetry and by electron-spray mass spectrometry (calculated molecular mass 1630 Daltons, determined 1629.55).

*Fluorescence Measurements*—All fluorescence measurements from cell suspensions were made on a Fluorolog (SPEX) spectrofluorimeter equipped with a 450 watt Xe lamp, a double grating excitation monochromator, and a single grating emission monochromator. Slits were set to 4 or 6 mm yielding bandwidths of 7.2 or 10.8 nm at excitation and 14.4 and 21.6 nm at emission. Data were acquired with a photon counting photomultiplier (linear up to $10^7$ counts/sec). Unless otherwise stated, cell suspensions ($10^6$ cell/ml) were placed in a 1-ml cuvette with magnetic stirring and maintained at 21 °C in a thermostatted cuvette handler. Time-based recordings were typically sampled every 100 or 300 ms.

For intracellular calcium release responses, cells were loaded in culture medium supplemented with 5 $\mu$M Fura-2 AM (acetylmethylester), or Fura-Red AM for 30 min at 37 °C followed by a 15-min incubation in probe-free medium. Measurements were made in Hepes buffer with protease inhibitors at 21 °C. Fluorescence emission was detected at 510 nm (excitation 340 nm) for Fura-2, and at 610 nm (excitation 488 nm) for Fura-Red.

*Estimation of Donor-Acceptor Separation*—$E$, the efficiency of energy transfer, and Ro, the distance at which energy transfer from the donor (EGFP) to the acceptor (Bodipy) is half-maximal, were estimated as described previously (61). Ro is given by the equation: $Ro = (J\,K^2\,Q_o\,n^{-4})^{1/6} \times 9.7 \times 10^3$ Å, where $K^2$ is taken as 2/3 and $n$ as 1.4. The quantum yield $Q_o$ = 0.66 of EGFP is taken from the literature (35). From the calculated overlap integral for the combined emission of EGFP and absorbance of Bodipy ($J = 3.14 \times 10^{-13}$ cm$^3$ M$^{-1}$), the Ro value was estimated to be 52.6 Å for NKA-Bo. Donor-acceptor separation is given by $r = [(E^{-1}) - 1]^{1/6}$ Ro, where $E$, the maximal efficiency of energy transfer, given by $E = 1 - (F_{DA}/F_D)$, was determined by measuring specific donor fluorescence emission in the presence ($F_{DA}$) and absence ($F_D$) of ligand at saturating concentrations (100 nM) of NKA-Bo. Specific EGFP fluorescence in the absence ($F_D$) and presence ($F_{DA}$) of ligand was determined by subtracting autofluorescence of nontransfected cells from total fluorescence of chimera 1 expressing cells (after selection with 0.5 mg/ml hygromycin, 40% of total initial fluorescence is due to cell autofluorescence).

*Single Cell Recordings and Confocal Microscopy*—NKA-Bo binding and intracellular calcium responses were measured from adherent HEK cells grown on glass coverslips and incubated in Ringer solution (140 mM NaCl, 5 mM KCl, 2 mM $MgCl_2$, 2 mM $CaCl_2$, 10 mM Hepes, 11 mM glucose, pH 7.3) at room temperature in the dark, using an inverted microscope (Nikon Eclipse TE300) equipped with a confocal imaging system (Bio-Rad MRC 1024 ES). Cells were first loaded with Fura-Red-AM (5 $\mu$M) for 30 min at 37 °C followed by a 15-min washout of the probe. Images were taken with a Plan Apo 40x oil immersion objective (Nikon). Excitation light (488 nm) was obtained using 1 or 3% power from a 30-milliwatt Kr-Ar laser. Emitted fluorescence was recorded at 522 ± 15 nm and 605 ± 22 nm and was color coded (256 gray levels). Images were acquired from a section located 3–6 $\mu$m above the glass coverslip at 2–4 Hz and analyzed using Bio-Rad time course software. Agonist was locally applied using pressurized (10 kilopascal) puffer pipettes (1–2 $\mu$m diameter) positioned 2–6 $\mu$m from the cell. Unless otherwise stated, the puffer pipette contained 200 nM NKA-Bo.

## RESULTS

*Construction of Fluorescent Chimeric NK2 Receptors and Neurokinin A*—Site-directed mutagenesis and ligand binding studies of NK2 tachykinin receptors (13, 14), as well as photoaffinity labeling of NK1 receptors using *p*-benzoyl-*p*-phenylalanine-substance P (15, 16), have provided strong support to the notion that tachykinins bind to extracellular domains of their respective receptor isotypes (17). To detect the interaction of neurokinin A with the NK2 receptor by fluorescence resonance energy transfer, we prepared two complementary DNA constructs joining the carboxyl terminus of EGFP to the hydrophilic amino-terminal part of the NK2 receptor at positions 15 (chimera 1) and 33 (chimera 2). As EGFP is not secreted by cells and according to the known extracellular location of the amino-terminal end of G protein-coupled receptors, the amino-terminal end of EGFP was further fused to the first 31 residues of the nicotinic receptor $\alpha$7 subunit (18) comprising a signal peptide to promote translocation of the amino-terminal domain to the extracellular space.

Neurokinin A was chemically derivatized by reaction of the amino group of its amino-terminal histidine residue with the fluorescent group Bodipy 530/550 iodoacetate, to yield a fluorescent mono-derivative, NKA-Bo. From the overlap between the absorbance spectrum of the Bodipy group and the emission spectrum of EGFP a theoretical Ro value of 52.6 Å was calculated. Energy transfer is thus expected to occur with more than 10% efficiency if the Bodipy group linked to NKA, and EGFP linked to the NK2 receptor are separated by 35–75 Å.

On transfection into HEK 293 cells, cDNAs encoding chimera 1 and 2 lead to the expression of fluorescent proteins exhibiting the characteristic excitation and emission spectra of EGFP. However, only chimera 1 yielded surface $^{125}$I-labeled neurokinin A binding sites sensitive to the competitive antagonist SR48968 (not shown) and was therefore used in further studies.

On confocal micrographs, chimera 1 decorates plasma membranes in HEK 293 cells (Fig. 1*A*). After incubation of the cells with 10 $\mu$M neurokinin A for 30 min at 37 °C, spots of intense fluorescence are detected at the plasma membrane, as well as on each confocal cross-section through the cell (Fig. 1*B*), strongly suggesting that receptor capping and internalization takes place after agonist exposure. On the other hand, preincubation with 10 $\mu$M of the competitive antagonist SR48968 results in a chimera 1 fluorescence distribution comparable to that of control (Fig. 1*C*).

*Functional and Pharmacological Properties of Fluorescent Chimera 1*—As shown in Fig. 1*D*, the addition of 10 nM NKA or 10 nM NKA-Bo to chimera 1 expressing HEK 293 cells loaded with the calcium indicator Fura-2 results in a typical intracellular calcium elevation response. These responses are not detected from nontransfected cells and are blocked by preincubation with the NK2-selective nonpeptide antagonist SR48968 (1 $\mu$M; Fig. 1*D*) as well as by the peptide antagonists cyclo(Gln-Trp-Phe-Gly-Leu-Met) (5 $\mu$M) or MEN-10,376 (10 $\mu$M).

Equilibrium binding studies reveal that [$^3$H]SR48968 interacts with saturatable binding sites on cells expressing either

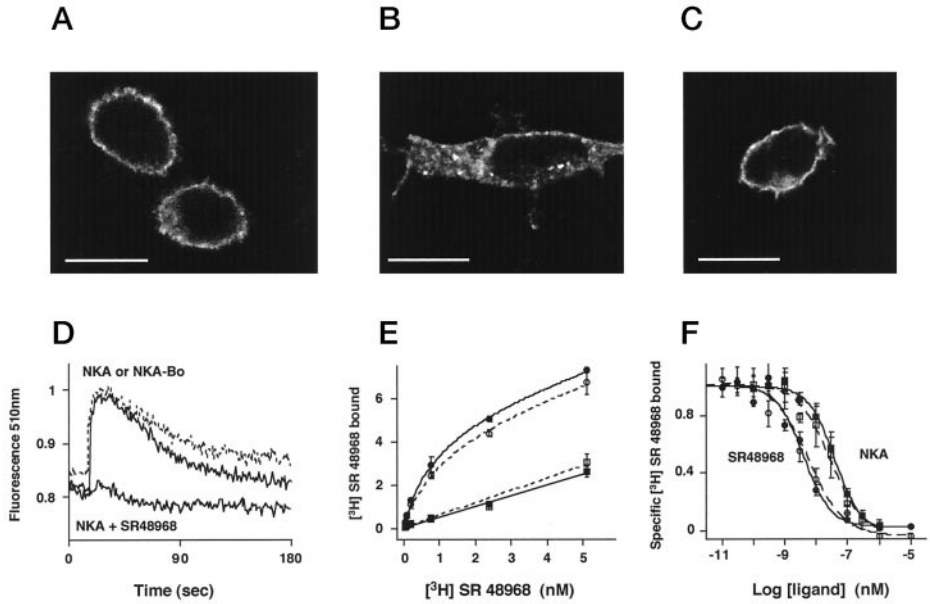


FIG. 1. **Expression and pharmacological characterization of chimera 1.** *A–C,* fluorescence confocal micrographs showing a section through the middle of formaldehyde-fixed HEK 293 cells stably expressing chimera 1, in the absence of ligand (*A*), after a 30-min incubation at 37 °C with 10 $\mu$M NKA (*B*), or 10 $\mu$M SR48968 and 10 $\mu$M NKA (*C*). EGFP fluorescence (white signal) was detected using the excitation and emission filters for fluorescein. Scale bars represent 10 $\mu$m. *D,* intracellular calcium release response recorded from Fura-2-loaded HEK 293 cells expressing chimera 1 stimulated with 10 nM NKA (*continuous lines*) or 10 nM NKA-Bo (*broken line*). Responses were recorded at 510 nm with excitation at 340 nm. NKA response evoked from chimera 1 expressing cells was blocked by SR48968. Fluorescence is expressed as counts/sec ($\times 10^{-7}$). *E,* [$^3$H]SR48968 binding (in dpm $\times 10^{-3}$) to WT NK2 (*filled symbols*) and chimera 1 (*open symbols*) expressing cells in suspension. Nonspecific binding was determined in the presence of 10 $\mu$M NKA. Each point is the mean ± S.D. of three independent determinations done in duplicate. *F,* inhibition of [$^3$H]SR48968 binding to WT NK2 (*filled symbols*) and chimera 1 (*open symbols*) expressing cells by SR48968 and NKA. Each point is the normalized mean ± S.D. of three independent determinations done in duplicate.

WT receptor or chimera 1 (Fig. 1*E*). Fusion of the NK2R with EGFP does not affect [$^3$H]SR48968 affinity (WT, $K_D$ = 0.92 ± 0.13 nM; chimera 1, $K_D$ = 0.98 ± 0.17 nM) nor the number of chimera 1 sites ($B_{max}$ = 0.1 pmol/25,000 cells, about 2 × $10^6$ receptors expressed/cell) as compared with WT NK2 receptor ($B_{max}$ = 0.08 pmol/25,000 cells).

Inhibition of [$^3$H]SR48968 binding to WT receptor and chimera 1 (Fig. 1*F*) by the agonist NKA (WT, $K_i$ = 64 ± 10 nM; chimera 1, $K_i$ = 64 ± 25 nM; $n$ = 3) or by the antagonist peptide MEN-10,376 (WT, $K_i$ = 53 ± 18 nM, $n$ = 3; chimera 1, $K_i$ = 62 ± 32 nM, $n$ = 3; not shown) also indicates that fusion of EGFP to the NK2 receptor does not significantly alter its pharmacological properties. Inhibition of [$^3$H]SR48968 binding to WT NK2R and chimera 1 by the fluorescent neurokinin A derivative, NKA-Bo, again reveals no difference between the two receptors (WT, $K_{iNKA-Bo}$ = 19.0 ± 3.5 nM; chimera 1, $K_{iNKA-Bo}$ = 16.6 ± 5.7 nM, $n$ = 3, data not shown) and shows that NKA-Bo exhibits about 3-fold higher equilibrium affinity than NKA.

When tested for competition against [$^{125}$I]NKA binding, both NKA and NKA-Bo exhibit higher apparent affinity (chimera 1, $K_{iNKA}$ = 1.5 ± 0.5 nM; chimera 1, $K_{iNKA-Bo}$ = 1.0 ± 0.7 nM) than when tested in competition against [$^3$H]SR48968, as has been described on cells expressing WT NK2 receptors (14). Thus, both the fluorescent NK2 receptor and the fluorescent neurokinin A derivative exhibit pharmacological and functional properties practically identical to those of their unmodified counterparts and therefore validate attempts to detect their interaction via fluorescence resonance energy transfer.

*Detection and Quantification of Receptor-Ligand Interactions by Fluorescence Resonance Energy Transfer on Living Cells*—Fluorescence resonance energy transfer experiments were carried out by exciting a cell suspension at the EGFP excitation wavelength (460–470 nm) and measuring either reduction of EGFP emission (at 510 nm) or an increase of emission of the Bodipy group (at 550 nm) (Fig. 2*A*). As illustrated in Fig. 2*B*, the addition of 23 or 46 nM NKA-Bo to a suspension of $10^6$ cells/ml expressing chimera 1 results in a progressive decrease in EGFP emission (at 510 nm) and a progressive increase in Bodipy emission (at 550 nm). Further addition of an excess of unlabeled NKA (10 $\mu$M), of SR48968 (20 $\mu$M), or MEN-10,376 (20 $\mu$M) fully restores EGFP emission to its initial level and partially reduces emission at the wavelength of the Bodipy group (Fig. 2*C*).

To ascertain that the observed fluorescence changes are because of energy transfer, the excitation spectrum of the donor was recorded at the emission of the acceptor. Indeed, excitation spectra (410–530 nm) monitored at Bodipy emission (570 nm) in the presence of 23 nM NKA-Bo and in the presence of 23 nM NKA-Bo together with 10 $\mu$M SR48968 allowed the determination of a subtraction excitation spectrum (Fig. 2*D*), which superimposes well with the excitation spectrum of EGFP directly recorded at EGFP emission (550 nm) in the absence of any ligand. This experiment thus strongly supports that both reduction of EGFP emission and increase of NKA-Bo emission signals (Fig. 2*C*) are because of fluorescence resonance energy transfer.

Reduction of chimera 1 emission amplitude at 510 ± 22 nm is proportional to the concentration of added NKA-Bo. Fig. 3*A* shows that in a continuous recording mode, the amplitude of EGFP emission decrease reaches a plateau value for ligand concentrations beyond 60 nM. When excitation is set to 460 ± 11 nm, the maximal decrease of fluorescence is close to 30% of total fluorescence (Fig. 3*A*) for cells selected with 0.5 mg/ml hygromycin B. Maximal extinction was 40% when excitation was set to 470 ± 10 nm (Fig. 2*C*). A plot of chimera 1 emission amplitude changes *versus* NKA-Bo concentration (Fig. 3*B*) yields a binding curve that is best fit with a single category of sites ($n_H$ = 1.0 ± 0.1) and an apparent $K_D$ value of 8.85 ± 1.02 nM ($n$ = 8). This value is intermediate compared with the apparent affinities determined by competition against [$^3$H]SR

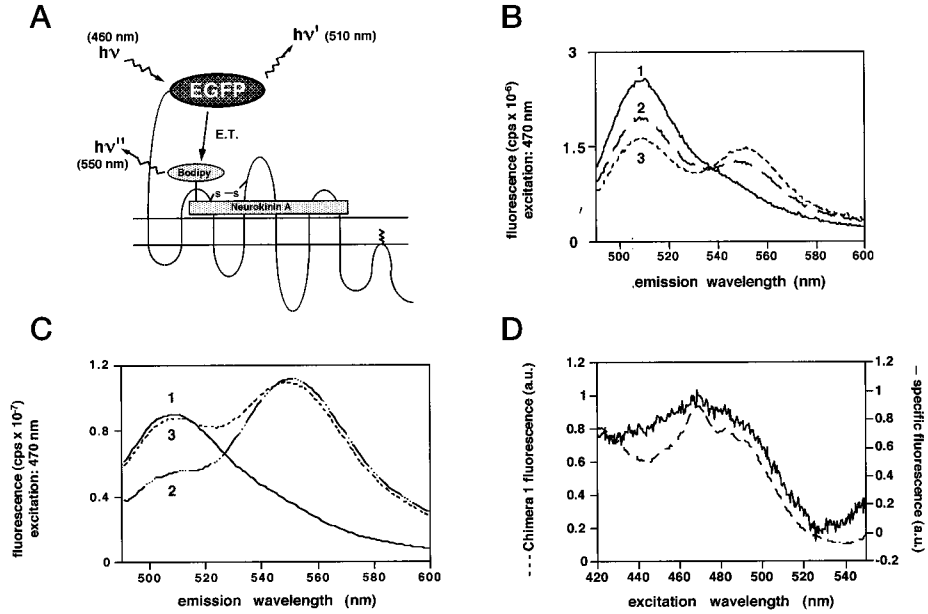


FIG. 2. **Detection of fluorescent Bodipy-labeled NKA (NKA-Bo) interaction with chimera 1 from HEK 293 cells in suspension.** *A,* schematic view of a chimera 1-NKA-Bo complex with excitation and emission wavelength used for fluorescence measurements. *E.T.,* energy transfer. *B,* fluorescence emission spectrum (excitation 470 nm) of a $5 \times 10^5$ cells/ml suspension of chimera 1 expressing cells in the absence (*trace 1*) or presence of 23 nm (*trace 2*) or 46 nm (*trace 3*) of NKA-Bo. Fluorescence is expressed as counts/sec (*cps*). *C,* reversibility of 100 nM NKA-Bo binding to chimera 1. Fluorescence emission spectra were sequentially recorded from a $2 \times 10^6$ cells/ml suspension of chimera 1 expressing cells (*trace 1*), after 2 min incubation with 100 nM NKA-Bo (*trace 2*), and after a further 10-min incubation with 20 $\mu$M SR48968. *D,* detection of chimera 1 fluorescence excitation spectrum at NKA-Bo fluorescence emission. The *continuous line* corresponds to the subtraction between an excitation spectrum recorded on a $5 \times 10^5$ cells/ml suspension incubated with 23 nM NKA-Bo and an excitation of the same preparation after further incubation with 10 $\mu$M SR48968 recorded at 570 nm. The excitation spectrum of chimera 1 alone (*broken line*) recorded at 550 nm is included for reference. Because of large amplitude differences between subtraction and control spectra, fluorescence is expressed in arbitrary units (*a.u.*).

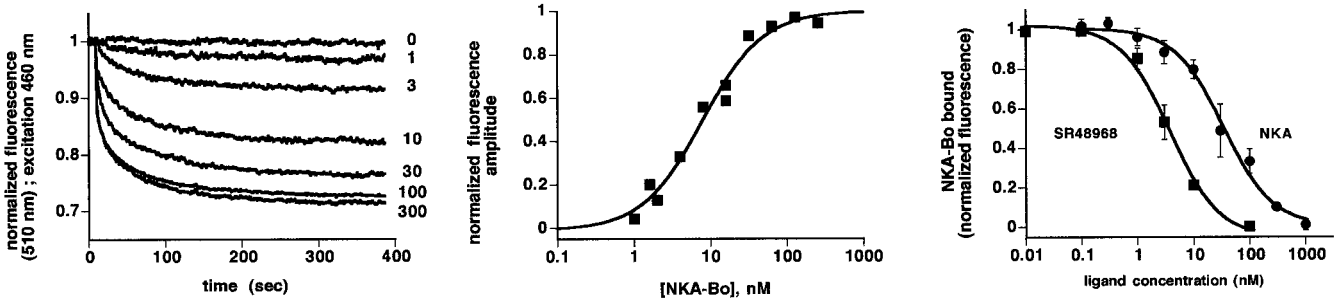


FIG. 3. **Pharmacological characterization of NKA-Bo binding to chimera 1 expressing HEK cells determined by fluorescence resonance energy transfer.** *A,* continuous recording of the reduction of chimera 1 fluorescence amplitude (510 nm) in the presence of various concentrations of NKA-Bo. Normalized traces correspond to individual recordings of a $10^6$ cell/ml suspension of chimera 1 expressing HEK 293 cells excited at 460 nm. NKA-Bo concentrations (in nM) are given next to each trace. The trace recorded at 300 nM NKA-Bo is corrected for the increment of 510 nm fluorescence resulting from Bodipy group emission. *B,* representative NKA-Bo binding curve to chimera 1. Each point corresponds to a normalized single determination of the reduction of chimera 1 fluorescence amplitude, as measured in *A* at equilibrium, plotted as a function of added NKA-Bo. The *solid line* corresponds to the best fit of the data to the empirical Hill equation derived for saturation. *C,* inhibition of NKA-Bo binding to chimera 1 by SR48968 and NKA was determined on a suspension of chimera 1-expressing cells preincubated with the given concentration of nonfluorescent ligand. After the addition of 8–10 nM NKA-Bo, fluorescence emission at 510 nm (excitation 460 nm) was determined until equilibrium was reached. Each data point represents the mean ± S.D. amplitude of the chimera 1 emission decrease as compared with a control. The *solid line* corresponds to the best fit of the data points to the empirical Hill equation derived for competition.

48968 and [$^{125}$I]NKA and presumably reflects binding of NKA-Bo to two conformations of the receptor.

When NKA-Bo concentration is set to its apparent $K_D$ value, NKA and SR48968 inhibit NKA-Bo binding to chimera 1 (Fig. 3*C*) with apparent inhibition constant values of 27.7 ± 6.0 nM ($n = 5$) and 1.7 ± 0.1 nM ($n = 5$), respectively.

*Sensitivity of Ligand-Receptor Complex Detection*—Steady-state receptor-ligand interactions were typically monitored in a 1-ml cuvette with irradiation and observation windows (3 × 10 mm) such that the efficacious volume of the cell suspension was 90 $\mu$l. At a standard cell concentration ($10^6$ cells/ml), the fluorescence signal was thus statistically recorded from 90,000 cells. To test for detection sensitivity, the cell concentration was decreased to 250,000 and 100,000 cells/ml. Taking the lowest cell concentration (100,000 cells/ml) as reference, initial chimera 1 fluorescence was found to increase by 2-fold at 250,000 cells/ml and by 8-fold at 1,000,000 cells/ml, in agreement with the notion that the efficacious irradiated and recorded sample volume decreases because of light scattering. However, at all cell concentrations, the addition of 60 nM NKA-Bo caused a specific reversible 30% reduction of EGFP emission amplitude (excitation 460 ± 11 nm, data not shown). The interaction between chimera 1 and NKA-Bo can thus be recorded in a standard spectrofluorimeter from a minimum of about 10,000 cells and represents a fixed proportion of total fluorescence, thus allowing to determine the fraction of receptors occupied independently of cell concentration.

*Single Cell Recording of Ligand Binding and Intracellular*

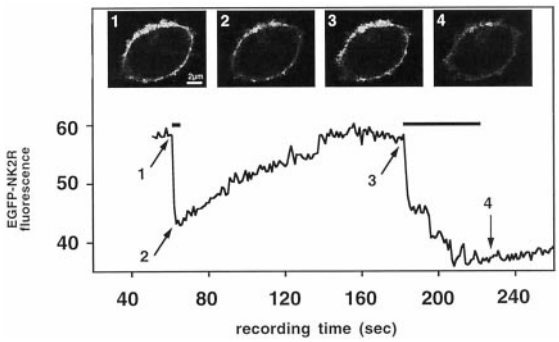


FIG. 4. **NKA-Bo binding to a single chimera 1 expressing HEK cell (selected with 0.5 mg/ml hygromycin B).** The puffer pipette contained 2 $\mu$M NKA-Bo and was positioned at about 4 $\mu$m from the top of the cell. Application durations depicted by *bars* were 1 s (first) and 40 s (second). The *solid line* represents time course of fluorescence intensity (in arbitrary units) from the whole plasma membrane area. Confocal micrographs 1 and 3 were taken before first and second applications, respectively; images 2 and 4 were taken at maximal fluorescence extinction during each ligand application.

*Calcium Elevation*—Observation of single cell fluorescence by confocal microscopy reveals that NKA-Bo application results in a decrease of receptor fluorescence in a reversible manner (Fig. 4). This reduction exhibits dose dependence with NKA-Bo concentration and does not occur when an excess of SR48968 is applied together with fluorescent agonist (not shown). As observed on cell suspensions, saturating concentrations of fluorescent agonist (200 nM-2 $\mu$M) lead to a maximal fluorescence extinction of 37.5 ± 2.5% ($n$ = 20, selection with 0.5 mg/ml hygromycin B). When cells were selected with 4 mg/ml hygromycin B, maximal extinction was 47.5 ± 3% ($n$ = 10, not shown). Quantification of fluorescence extinction thus allows to determine the fraction of receptors occupied and as a consequence the effective ligand concentration at the membrane. For instance, for the cell shown in Fig. 4, the first ligand application (2 $\mu$M, during 1 s) leads a 25% decrease of fluorescence, thus to about 66% occupancy of receptor sites. From the NKA-Bo saturation curve (Fig. 3*B*), the effective ligand concentration at receptors can be estimated to be about 10 nM. After application, NKA-Bo dissociates from its binding sites at a rate ($k_{off}$ = 0.016 $s^{-1}$) almost identical to that determined on cell suspensions ($k_{off}$ = 0.018 $s^{-1}$, not shown). The second application (40-s pulse) results in 37% extinction of fluorescence and reflects saturation of receptor sites.

Calcium responses were also recorded in parallel to ligand binding. A first local NKA-Bo application (1 $\mu$M, 5 s) to the cell shown in Fig. 5*A* leads to a large calcium response. Ligand binding analysis reveals that the receptor fluorescence in the area facing the tip of the application pipette ("east" side of the cell) rapidly decreases by 15.5% (*i.e.* 40% of receptor sites are occupied). A second application (1 $\mu$M, 5 s) of NKA-Bo to the same location, 4.5 min after the first application, does not lead to any detectable calcium response, although more than 50% of receptor sites was not occupied during the first application. Such ligand application to a given pole of a cell followed by a second application to the same pole never led ($n$ = 20) to a second calcium response.

Two approaches were used to test whether calcium release machinery was desensitized or whether receptors were no longer able to couple to intracellular effectors. First, NKA 4–10, a truncated, nondesensitizing version of NKA, was utilized. Successive applications of NKA 4–10 to NK2R expressing oocytes have been shown to trigger repetitive responses (19), whereas NKA only led to a single response. Here, in agreement, repeated applications of NKA 4–10 (10 $\mu$M, 5 s) to HEK cells expressing chimera 1 lead to repetitive intracellular calcium

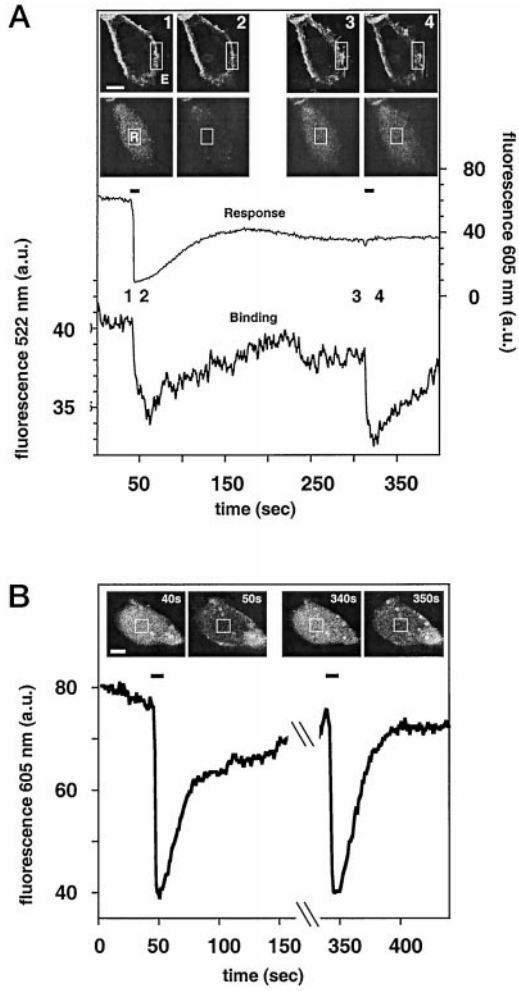


FIG. 5. *A,* simultaneous measurement of NKA-Bo binding and intracellular calcium responses from a single cell (selected with 4 mg/ml hygromycin B). Ligand binding was recorded from the indicated membrane area at the east pole (*E*) as EGFP fluorescence decrease at 522 nm (arbitrary units, *upper row* of images, scale bar 2 $\mu$m), and calcium elevation was recorded from the indicated response area (*R*) as Fura-Red fluorescence decrease at 605 nm (arbitrary units, *lower row* of images). The puffer pipette contained 1 $\mu$M NKA-Bo and was placed facing the boxed membrane area at a distance of about 4 $\mu$m. NKA-Bo was applied for 5 s at time 45 and 315 s (*horizontal bars*). Amplitudes of receptor fluorescence decrease is 15% during the first ligand application and 13% during the second ligand application, which correspond to 40 and 35%, respectively, receptor occupancy. Note the lack of calcium response to the second agonist application. *B,* absence of response desensitization to successive applications of NKA 4–10. Intracellular calcium rises in a single HEK cell expressing chimera 1 were measured using Fura-Red (605-nm emission) after puffer applications of 10 $\mu$M NKA 4–10 (5 s) separated by a 6-min washout. Images were taken at the indicated times; the time course of Fura-Red fluorescence measured from the response area is shown below.

elevations (Fig. 5*B, n* = 5) unlike NKA (10 $\mu$M), which never activated a second response (not shown). Second, to further investigate the relationship between receptor site occupancy by NKA-Bo and development of calcium responses, the duration of perfusion pulses was reduced to 3 s to favor local application at one pole of the cell only. Under such conditions, intracellular calcium elevation initiates from limited ligand binding (27% occupancy) to the north pole without detectable receptor occupancy at the south pole (Fig. 6*A–C*). A second short application (3 s) carried out 6 min later at the same pole resulted in no or a negligibly small response. However, application of ligand to the south pole of the same cell (Fig. 6, *D–F*) leads to a calcium response resulting from ligand binding to 30% of the south pole

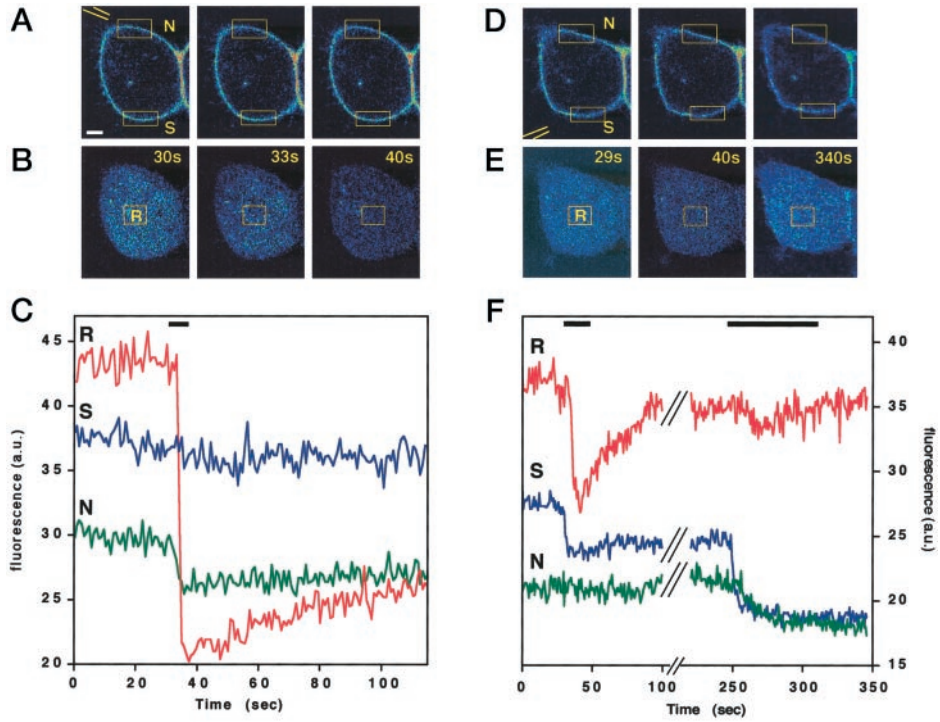


FIG. 6. **Selective local applications of NKA-Bo and measurements of ligand binding and intracellular calcium from a single cell (selected with 0.5 mg/ml hygromycin B).** Ligand binding was recorded from the indicated (*N, green line* and *S, blue line*) membrane areas as EGFP fluorescence decrease at 522 nm (arbitrary units, *upper row* of images, scale bar 2 $\mu$m), and calcium elevation was recorded from the indicated response area (*R, red line*) as Fura-Red fluorescence decrease at 605 nm (arbitrary units, *lower row* of images). The puffer pipette contained 200 nM NKA-Bo and was placed as indicated in the images; agonist was applied at each pole for 3 s. Because of a change of cell shape between application at north pole and application at south pole, areas of quantification were defined for each recording, therefore accounting for slight changes in initial fluorescence levels. *A–C,* agonist application at the north pole. Ligand rapidly binds to the *N* area and initiates a calcium response with a 2-s delay but does not reach the *S* area. Images were taken 1 s before ligand application (30 s), 2 s after the beginning of perfusion (33 s), and 9 s after the beginning of perfusion (40 s). *D–F,* agonist application at the south pole of the same cell 6 min after the initial application at the north pole. Ligand binding to *S* pole receptors initiates a calcium response without measurable *N* pole receptor occupancy. A subsequent long duration application (90 s) leads to saturation of receptor sites at the *S* pole and partial occupancy of sites at the *N* pole with a very weak calcium response. Images were taken 1 s before (29 s) and 10 s after (40 s) the first agonist application and after saturation of receptor sites by a 90 s application (340 s).

receptors with no detectable binding at the north pole. Further stimulation of the cell, with either short (0.5 s, not shown) or long (90 s) application to the same pole (Fig. 6, *D–F*), leads to further receptor occupancy up to saturation (fluorescence decrease at south pole: 35%, corresponding to 95% receptor occupancy) but with significantly reduced or undetectable calcium responses ($n = 7$) even after several minutes of delay between applications. Taken together, these data demonstrate that the inability of cells to respond to a second NKA-Bo application 4–6 min after the first application is not because of desensitization of the calcium release machinery but rather that it is because of exposure of receptor sites to agonist and thus presumably to homologous and/or heterologous desensitization.

In contrast to NK1 receptors (20), NK2 receptors have not yet been firmly shown to be regulated by G protein receptor kinases, although indirect evidence supports this view (19). NK2 receptors are on the other hand well known to be regulated via desensitization involving activation of protein kinase C by the second messengers calcium and diacylglycerol, produced by phospholipase C (9, 21). When HEK cells expressing WT NK2 receptors are transfected with PKC$\alpha$-EGFP, application of NKA stimulates PKC$\alpha$ translocation to the plasma membrane (Fig. 7*A*) and intracellular calcium elevation (Fig. 7*B*). Local agonist application leads to rapid and reversible PKC translocation to the plasma membrane (as seen in Fig. 7*A,* recording area 4). Analysis of the time course of PKC translocation (Fig. 7*C*) reveals that PKC rapidly but transiently migrates to the whole perimeter of the cell (areas 2–4). It then redistributes to a longer lasting membrane-bound form that accumulates at the pole exposed to agonist (Fig. 7*A*, area 4) with a return to initial conditions within 1 min following agonist application (Fig. 7*C*).

## DISCUSSION

Since the identification of G protein-coupled neurotransmitter receptors, many proteins involved in the regulation of the responses mediated by these receptors have been identified and their biochemical roles characterized (4, 7). It is now also well established that stimulation of one defined receptor isotype may trigger several response pathways, depending for instance on the agonist (22), on the cell type (21, 23), on the dose or duration of agonist application (24, 25), or on sequential interaction with intracellular effectors (26). Although several experimental approaches have been developed to better understand, in a dynamic manner, the relationships between the receptors, their ligands, and their effectors (27–31), new tools are still needed to improve detection sensitivity, temporal resolution, and to allow investigation on intact cells.

The recent isolation (32), identification, structural resolution (33, 34), and engineering of the gene encoding jellyfish autofluorescent proteins (35), the green fluorescent protein, and its mutants, has led to the development of new tools to label proteins and to investigate their expression (36), trafficking (37), subcellular distribution (38), homophilic or heterophilic interactions (39), or to monitor structural or conformational changes (40).

As a step toward developing sensitive detection methods applicable to G protein-coupled neurotransmitter receptors, we

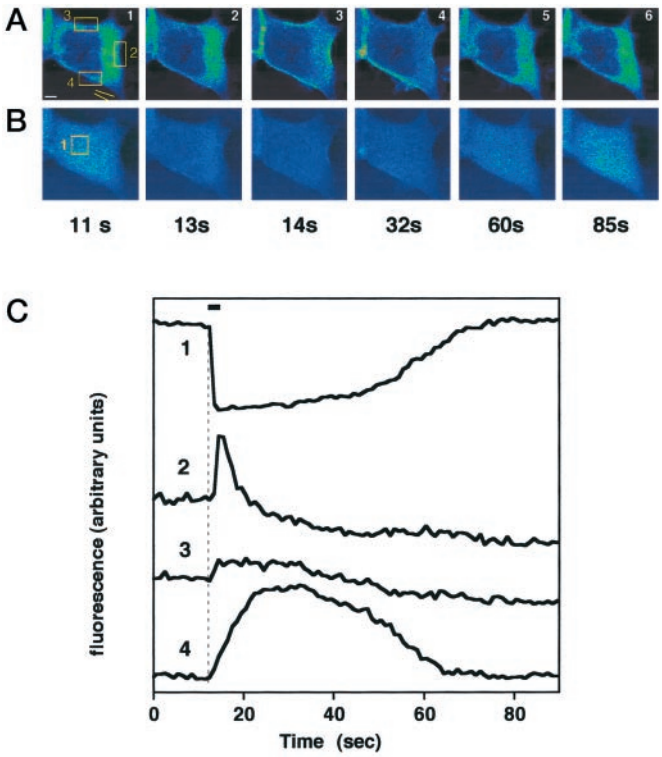


FIG. 7. **Translocation of PKC$\alpha$-EGFP after stimulation of WT NK2 receptor expressing HEK 293 cells.** *A–B,* PKC$\alpha$ fluorescence was recorded from the indicated membrane areas as EGFP fluorescence at 522 nm (*A*, arbitrary units, *upper row* of images) and calcium elevation was recorded from the indicated response area (*1*) as Fura-Red fluorescence decrease at 605 nm (*B*, arbitrary units, *lower row* of images). The puffer pipette contained 1 $\mu$M NKA and was positioned facing area 4 as indicated in image 1; agonist was applied for 1 s. Images shown (scale bar 2 $\mu$m) are taken 1 s before application (11 s, application was at 12 s) and at the indicated times after (13 s, peak of response; 14 s, beginning of PKC translocation; 32 s, concentration of PKC in area 4; 60 and 85 s, return to basal level). *C,* time course of changes in PKC$\alpha$-EFGP fluorescence (from membrane areas 2–4) and Fura-Red fluorescence from the response area 1.

use EGFP to genetically label the NK2 receptor in a quantitative and homogeneous manner. EGFP was linked to the amino-terminal end of the NK2 receptor, rather than to the carboxyl terminus, for two reasons. First, green fluorescent protein is a substrate of cAMP-dependent protein kinases in mammalian cells (41), and phosphorylation of green fluorescent protein is accompanied by a two-fold increase of fluorescence emission. Because NK2 receptors may stimulate cAMP production, as shown in Rat-1 cells (21), a phosphorylation-associated change in intrinsic green fluorescent protein fluorescence may interfere with the recording of the desired ligand-receptor interaction signal. Second, the calculated Ro value (in the 50 Å range) for energy transfer between EGFP and the Bodipy group indicates that energy transfer can reasonably be measured between fluorophores located on the same side of the plasma membrane. However, it is unlikely, given the size of EGFP ($50 \times 30$ Å) and thickness of the lipid bilayer (40–60 Å), that efficient energy transfer will take place from one side of the bilayer to the other.

We find that fusion of EGFP at the amino-terminal end of the NK2 receptor is an efficient way to label the receptor without altering its properties. Indeed, the expression level of chimera 1 is similar to that of wild type receptors, and confocal micrographs confirm that the fluorescent protein is correctly targeted to the plasma membrane compartment. Also, agonist- and antagonist-binding properties, as well as coupling of the mutant receptor to intracellular calcium responses and long term regulation of response desensitization, are comparable, if not identical, to those of the wild type receptor. Such absence of changes in the pharmacological and physiological properties of receptors may be general, as similar tagging of the human muscarinic M1 receptor has been also found to yield a fully functional membrane-bound protein (42, 43).

Neither EGFP nor Bodipy appear to behave as conformation-sensitive probes in the present context. Indeed, activation of chimera 1 with NKA is not accompanied by EGFP fluorescence changes, and activation of WT receptor with NKA-Bo also does not result in any fluorescence change of the Bodipy group. Thus, EGFP and Bodipy are likely to freely reorientate, without experiencing changes in their environment, in the unbound and bound forms of the receptor and the ligand, and serve as conformation-independent reporters of receptor-ligand interactions.

NKA-Bo binding is best detected and quantified by measuring extinction of EGFP emission, because at the Bodipy emission wavelength, a significant emission resulting from direct excitation of Bodipy at 460–470 nm is detected. Interestingly, for saturating ligand concentrations, EGFP fluorescence extinction reaches a maximal amplitude that is reproducible between cell batches (37% for cells selected with 0.5 mg/ml hygromycin B and 47% at 4 mg/ml). Thus, as for cell suspensions, effective ligand concentration at the membrane and receptor occupancy can be quantified on single cells. As shown here, direct detection of receptor occupancy allows the estimation of ligand diffusion and thus exposure of receptors to the effective ligand concentration with high spatial resolution.

As previously shown with NKA (19), NKA-Bo leads to rapid and long-lasting desensitization of cellular responses, which contrasts with the nondesensitizing responses elicited by the truncated neurokinin, NKA 4–10. Desensitization of NKA-Bo responses is pronounced at membrane areas exposed to agonist and takes place at concentrations that do not saturate receptor sites. Homologous desensitization, *i.e.* desensitization of receptor molecules activated by agonist, thus may not represent the sole regulatory pathway accounting for the profound desensitization to NKA-Bo.

NK2 receptors are well known to be regulated via desensitization involving protein kinase C (21). The present work shows that PKC$\alpha$ translocation to the membrane is more pronounced and lasts much longer at the pole of the cell exposed to NKA-Bo than at the other poles. This is in agreement with observations made on the tumor mast cell line 2H3 showing that calcium elevation is sufficient to promote PKC translocation to the membrane but not activation, which requires the additional presence of diacylglycerol (9, 44). The present data further suggest that the long lasting translocation of PKC to the plasma membrane takes place in the vicinity of activated receptor molecules, where phospholipase C may selectively become active to locally produce diacylglycerol.

Consistent with the notion of subcellular compartmentalization of G protein-coupled receptor signal transduction regulation is the finding that several effectors of G protein-coupled receptors are localized to membrane microdomains (45–47), where receptor molecules (48–50) associate with heterotrimeric G proteins (51, 52), PKC isoforms (53, 54), and second messengers such as diacylglycerol (55). In such a scheme, compartmentalized desensitization of tachykinin receptors may take place in a pseudo-heterologous manner within membrane microdomains to which active PKC would be targeted and would phosphorylate not only agonist-bound forms of receptors but also unliganded receptor molecules. Therefore, similar to response activation and homologous desensitization, which both strictly depend on exposure to agonist and exhibit com-

partmentalization, heterologous desensitization could also develop in the vicinity of activated receptors.

In conclusion, the present work shows that receptor-ligand interactions at G protein-coupled receptors can be monitored and quantified by fluorescence resonance energy transfer, an approach that is compatible with live cells, and thus with preservation of intracellular effectors of the response and associated second messengers. Such interactions can be measured with high spatial resolution and followed in parallel with intracellular calcium response onset and decline to show compartmentalization not only of response activation but also of desensitization, including heterologous desensitization. Time-resolved measurement of ligand binding together with the monitoring of the activation of intracellular effectors should allow the further characterization of the pattern of interactions regulating cellular responses mediated by G protein-coupled receptors.

*Acknowledgments*— We thank F. Pattus, M.P. Reck, D. Bertrand, C. D. Muller, and T. Palanché for helpful comments, J. P. Loeffler for the confocal micrographs in Fig. 1, and S. Nakanishi, J. P. Changeux, and D. Joubert for plasmids.

REFERENCES

1. Changeux, J. P., Devillers-Thiéry, A., and Chemouilli, P. (1984) *Science* **225,** 1335–1345
2. Karlin, A. (1993) *Curr. Opin. Neurobiol.* **3,** 299–309
3. Galzi, J. L., and Changeux, J. P. (1994) *Curr. Opin. Struct. Biol.* **4,** 554–565
4. Lefkowitz, R. J. (1996) *Nature Biotechnol.* **14,** 283–286
5. Barak, L. S., Ferguson, S. S. G., Zhang, J., and Caron, M. (1997) *J. Biol. Chem.* **272,** 27497–27500
6. Gilman, A. G. (1987) *Annu. Rev. Biochem.* **56,** 615–649
7. Gudermann, T., Schoneberg, T., and Schultz, G. (1997) *Annu. Rev. Neurosci.* **20,** 399–427
8. Tsunoda, S., Sierralta, J., Sun, Y., Bodner, R., Suzuki, E., Becker, A., Socolich, M., and Zuker, C. S. (1997) *Nature* **388,** 243–249
9. Oancea, E., and Meyer, T. (1998) *Cell* **95,** 307–318
10. Cao, Y. Q., Mantyh, P. W., Carlson, E. J., Gillespie, A. M., Epstein, C. J., and Basbaum, A. I. (1998) *Nature* **392,** 390–394
11. De Felipe, C., Herrero, J. F., O'Brien, J. A., Palmer, J. A., Doyle, C. A., Smith, A. J. H., Laird, J. M. A., Belmonte, C., Cervero, F., and Hunt, S. P. (1998) *Nature* **392,** 394–397
12. Nakanishi, S., Nakajima, Y., and Yokota, Y. (1993) *Regul. Pept.* **46,** 37–42
13. Werge, T. M. (1994) *J. Biol. Chem.* **269,** 22054–22058
14. Huang, R. R. C., Vicario, P. P., Strader, C. D., and Fong, T. M. (1995) *Biochemistry* **34,** 10048–10055
15. Li, Y.-M., Marnerakis, M., Stimson, E. R., and Maggio, J. E. (1995) *J. Biol. Chem.* **270,** 1213–1220
16. Boyd, N. D., Kage, R., Dumas, J. J., Krause, J. E., and Leeman, S. E. (1996) *Proc. Natl. Acad. Sci. U. S. A.* **93,** 433–437
17. Schwartz, T. (1994) *Curr. Opin. Biotechnol.* **5,** 434–444
18. Couturier, S., Bertrand, D., Matter, J. M., Hernandez, M. C., Bertrand, S., Millar, N., Valera, S., Barkas, T., and Ballivet, M. (1990) *Neuron* **5,** 845–856
19. Nemeth, K., and Chollet, A. (1995) *J. Biol. Chem.* **270,** 27601–27605
20. McConalogue, K., Corvera, C. U., Gamp, P. D., Grady, E. F., and Bunnett, N. W. (1998) *Mol. Biol. Cell* **9,** 2305–2324
21. Alblas, J., van Etten, H., Khanum, A., and Moolenaar, W. H. (1995) *J. Biol. Chem.* **270,** 8944–8951
22. Varrault, A., and Bockaert, J. (1992) *Naunyn-Schmiedeberg's Arch. Pharmacol.* **346,** 367–374
23. Alblas, J., van Etten, I., and Moolenaar, W. H. (1996) *EMBO J.* **15,** 3351–3360
24. Di Marzo, V., Vial, D., Sokoloff, P., Schwartz, J. C., and Piomelli, D. (1993) *J. Neurosci.* **13,** 4846–4853
25. Daaka, Y., Luttrell, L. M., and Lefkowitz, R. J. (1997) *Nature* **390,** 88–91
26. Luttrell, L. M., Ferguson, S. S., Daaka, Y., Miller, W. E., Maudsley, S., Della Rocca, G. J., Lin, F., Kawakatsu, H., Owada, K., Luttrell, D. K., Caron, M. G., and Lefkowitz, R. J. (1999) *Science* **283,** 655–661
27. Breer, H., Boekhoff, I., and Tareilus, E. (1990) *Nature* **345,** 65–68
28. Fay, S. P., Posner, R. G., Swann, W. N., and Sklar, L. A. (1991) *Biochemistry* **30,** 5066–5075
29. Vuong, T. M., and Chabre, M. (1991) *Proc. Natl. Acad. Sci. U. S. A.* **88,** 9813–9817
30. Neubig, R. R., and Sklar, L. A. (1993) *Mol. Pharmacol.* **43,** 734–740
31. Posner, R. G., Fay, S. P., Domalewski, M. D., and Sklar, L. A. (1994) *Mol. Pharmacol.* **45,** 65–73
32. Prasher, D. C., Eckenrode, V. K., Ward, W. W., Prendergast, F. G., and Cormier, M. J. (1992) *Gene* (*Amst.*) **111,** 229–233
33. Ormö, M., Cubitt, A., Kallio, K., Gross, L. A., Tsien, R. Y., and Remington, S. (1996) *Science* **273,** 1392–1395
34. Yang, F., Moss, L. G., and Phillips, G. N., Jr. (1996) *Nature Biotechnol.* **14,** 1246–1251
35. Heim, R., and Tsien, R. Y. (1996) *Curr. Biol.* **6,** 178–182
36. Marshall, J., Molloy, R., Moss, G. W. J., Howe, J. R., and Hughes, T. (1995) *Neuron* **14,** 211–215
37. Tarasova, N. I., Stauber, R. H., Choi, J. K., Hudson, E. A., Czerwinski, G., Miller, J. L., Pavlakis, G. N., Michejda, C. J., and Wank, S. A. (1997) *J. Biol. Chem.* **272,** 14817–14824
38. Barak, L. S., Warabi, K., Feng, X., Caron, M. G., and Kwatra, M. M. (1999) *J. Biol. Chem.* **274,** 7565–7569
39. Periasamy, A., Kay, S. A., and Day, R. N. (1997) *Proc. Int. Soc. Optical Eng.* **2983,** 58–66
40. Miyawaki, A., Llopis, J., Heim, R., McCaffery, J. M., Adams, J. A., Ikura, M., and Tsien, R. Y. (1997) *Nature* **388,** 882–887
41. Thastrup, O., Tullin, S., and Poulsen, L. (August 8, 1996) International Patent WO 96/23898
42. Weill, C., Ilien, B., Goeldner, M., and Galzi, J. L. (1999) *J. Rec. Sign. Transd. Res.* **19,** 423–436
43. Weill, C., Galzi, J. L., Chasserot-Golaz, S., Goeldner, M., and Ilien, B. (1999) *J. Neurochem.* **73,** 791–801
44. Nishizuka, Y. (1992) *Science* **258,** 607–614
45. Simons, K., and Ikonen, E. (1997) *Nature* **387,** 569–572
46. Anderson, R. G. (1998) *Annu. Rev. Biochem.* **67,** 199–225
47. Brown, D. A., and London, E. (1998) *Annu. Rev. Cell Dev. Biol.* **14,** 111–136
48. Dupree, P., Parton, R. G., Raposo, G., Kurzchalia, T. V., and Simons, K. (1993) *EMBO J.* **12,** 1597–1605
49. Feron, O., Smith, T. W., Michel, T., and Kelly, R. A. (1997) *J. Biol. Chem.* **272,** 17744–17748
50. Feron, O., Han, X., and Kelly, R. A. (1999) *Life Sci.* **64,** 471–477
51. Sargiacomo, M., Sudol, M., Tang, Z., and Lisanti, M. P. (1993) *J. Cell Biol.* **122,** 789–807
52. Li, S., Okamoto, T., Chun, M., Sargiacomo, M., Casanova, J. E., Hansen, S. H., Nishimoto, I., and Lisanti, M. P. (1995) *J. Biol. Chem.* **270,** 15693–15701
53. Lisanti, M. P., Scherer, P. E., Vidugiriene, J., Tang, Z., Hermanowski-Vosatka, A., Tu, Y. H., Cook, R. F., and Sargiacomo, M. (1994) *J. Cell Biol.* **126,** 111–126
54. Smart, E. J., Foster, D. C., Ying, Y. S., Kamen, B. A., and Anderson, R. G. (1994) *J. Cell Biol.* **124,** 307–313
55. Liu, P., and Anderson, R. G. (1995) *J. Biol. Chem.* **270,** 27179–27185
56. Sasai, Y., and Nakanishi, S. (1989) *Biochem. Biophys. Res. Commun.* **165,** 695–702
57. Eiselé, J. L., Bertrand, S., Galzi, J. L., Devillers-Thiéry, A., Changeux, J. P., and Bertrand, D. (1993) *Nature* **366,** 479–483
58. Chen, C., and Okayama, H. (1987) *Mol. Cell. Biol.* **7,** 2745–2752
59. Cheng, Y. G., and Prusoff, W. H. (1973) *Biochem. Pharmacol.* **22,** 3099–4005
60. Emonds-Alt, X., Vilain, P., Goulaouic, P., Proietto, V., Van Broek, D., Advenier, C., Naline, E., Neliat, G., Le Fur, G., and Breliere, J. C. (1992) *Life Sci.* **50,** 101–106
61. Lakey, J. H., Baty, D., and Pattus, F. (1991) *J. Mol. Biol.* **218,** 639–653